

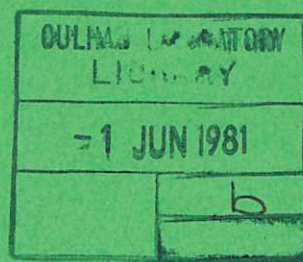


UKAEA

Preprint

A THEORY OF CURRENTS INDUCED BY RADIO-FREQUENCY WAVES IN TOROIDAL PLASMAS

J. G. CORDEY
T. EDLINGTON
D. F. H. START



CULHAM LABORATORY
Abingdon Oxfordshire

1981

This document is intended for publication in a journal or at a conference and is made available on the understanding that extracts or references will not be published prior to publication of the original, without the consent of the authors.

Enquiries about copyright and reproduction should be addressed to the Librarian, UKAEA, Culham Laboratory, Abingdon, Oxon. OX14 3DB, England.

A THEORY OF CURRENTS INDUCED BY RADIO-FREQUENCY WAVES IN TOROIDAL PLASMAS

J G Cordey, T Edlington and D F H Start
Culham Laboratory, Abingdon, Oxon OX14 3DB, UK
(Euratom/UKAEA Fusion Association)

ABSTRACT

A Fokker-Planck treatment of the plasma electron current driven by radio-frequency waves is presented for the electron cyclotron and Landau damping wave absorption mechanisms. Electron-electron collisions are taken into account using the full Fokker-Planck collision operator which leads to an integro-differential equation for the perturbation of the electron distribution function produced by the wave. This equation is solved analytically in the Lorentz gas approximation and numerically in its full form. Efficient current drive is predicted for high phase velocity waves in the electron cyclotron scheme while Landau damping is efficient at both high and low phase velocities. The reduction of the current due to trapping of electrons in a tokamak field configuration is calculated and a dramatic suppression of the current is predicted for low phase velocities. The efficiency of driving currents with waves is found to be comparable with that obtained using fast ion beams but much less than that using steady electric fields. A comparison with an idealised wave shows that the two practical schemes considered are far from optimum.

(Submitted for publication in Plasma Physics.)

March 1981
cms

1 INTRODUCTION

In 1971 Wort^[1] suggested that the plasma current of a tokamak reactor could be generated continuously using low frequency electromagnetic waves to drive the electrons by transit-time magnetic pumping. More recently Fisch and Karney^[2,3] have predicted that currents can also be driven efficiently by electron Landau damping of radio-frequency waves at both high and low phase velocities. An alternative to the Landau damping scheme has subsequently been proposed by Fisch and Boozer^[4] which relies on creating an asymmetric plasma resistivity rather than on transferring momentum to the electrons. In this scheme an electron cyclotron wave, for example, is used to increase the perpendicular energy of resonant electrons moving in a particular direction along the magnetic field lines. The reduced collisionality of these electrons leads to an asymmetry in the electron distribution function which manifests itself as a current.

In this paper a theory of wave driven plasma currents is presented both for the electron Landau damping scheme and for an asymmetric resistivity scheme which utilises electron cyclotron resonance heating. In section 2 the electron distribution function is determined for the case of a uniform magnetic field using a steady-state Fokker-Planck equation which includes electron-ion and electron-electron collisions together with the electron-wave interaction. The electron-electron collisions are treated using the full Fokker-Planck collision operator and, in this respect, the present method differs substantially from that in refs.2 and 3. The Fokker Planck equation is solved analytically in the Lorentz

gas approximation and numerically in its full form. Values of the current density per unit power density, J/P_d , are obtained for a wide range of wave phase velocity, several values of plasma charge, Z , and for the $\ell=1, 2$ and 3 harmonics of the electron cyclotron frequency.

In section 3 the reduction in current due to electron trapping in the toroidal field gradient of a tokamak is calculated. The results of the calculations both with and without electron trapping are compared in section 4 with the efficiencies of driving currents by means of an idealised, hypothetical radio-frequency wave, various types of ion beam and a steady electric field.

2 THE ELECTRON DISTRIBUTION FUNCTION

(a) The Fokker Planck Equation

The interaction between the plasma electrons and a radio-frequency wave produces a time development of the distribution function which can be written symbolically as

$$\frac{\partial f_e}{\partial t} = \left(\frac{\partial f_e}{\partial t} \right)_w + \left(\frac{\partial f_e}{\partial t} \right)_c \quad (1)$$

where $\left(\frac{\partial f_e}{\partial t} \right)_w$ represents the velocity space diffusion caused by the wave and $\left(\frac{\partial f_e}{\partial t} \right)_c$ is the Coulomb collision term. Using quasi-linear theory applied to a plasma in a uniform magnetic field Kennel and Engelmann^[5] have deduced a general expression for $\left(\frac{\partial f_e}{\partial t} \right)_w$ which, for a transverse electron wave with a wavelength much greater than the electron Larmor radius ($k_\perp, k_\parallel \ll \frac{\omega_c}{v_\perp}$), reduces to

$$\left(\frac{\partial f_e}{\partial t} \right)_w = \frac{1}{v_\perp} \frac{\partial}{\partial v_\perp} \left[D_c v_\perp^{2\ell-1} \delta \left(\frac{\omega - \ell \omega_c}{k_\parallel} - v_\parallel \right) \frac{\partial f_e}{\partial v_\perp} \right]. \quad (2)$$

In the above equation v_{\perp} and v_{\parallel} are the electron perpendicular and parallel velocities, D_c is a constant in velocity space and is proportional to the wave amplitude squared, ω and ω_c represent the wave frequency and the electron gyro-frequency respectively and k_{\parallel} is the wave vector along the magnetic field. The diffusion term for the electron Landau damping case is given by^[3]

$$\left(\frac{\partial f_e}{\partial t}\right)_w = \frac{\partial}{\partial v_{\parallel}} \left[D_L \delta \left(\frac{\omega}{k_{\parallel}} - v_{\parallel} \right) \frac{\partial f_e}{\partial v_{\parallel}} \right]. \quad (3)$$

In the present calculation the wave amplitude is assumed to be sufficiently small to produce only a small perturbation of the electron distribution function which can be written

$$f_{eo} = F_m + f'_{eo} \quad (4)$$

where F_m is the Maxwellian distribution and the zero subscript denotes no trapped electrons. Equation (1) can then be linearised giving, for the electron cyclotron wave in steady state

$$\begin{aligned} \frac{1}{v_{\perp}} \frac{\partial}{\partial v_{\perp}} \left[D_c v_{\perp}^{2\ell-1} \delta \left(\frac{\omega - \ell \omega_c}{k_{\parallel}} - v_{\parallel} \right) \frac{\partial F_m}{\partial v_{\perp}} \right] + C_{ei}(f'_{eo}, F_m) + C_{ee}(f'_{eo}, F_m) \\ + C_{ee}(F_m, f'_{eo}) = 0. \quad (5) \end{aligned}$$

In eq(5), C symbolises the Fokker-Planck collision operator. In order to solve eq(5) (and the equivalent equation for Landau damping) a Legendre polynomial expansion of the perturbation of the distribution is made:

$$f'_{e0} = F_m \sum_n a_n(v) P_n(\xi) \quad (6)$$

where $\xi = v_{||}/v$.

Substituting eq(6) into eq(5) leads to the following integro-differential equation for a_1 , the coefficient which determines the electron current:

$$a_1'' + P(x)a_1' + Q(x)a_1 - \frac{16}{3\pi^{\frac{1}{2}}\Lambda} \left[xI_3(x) - 1.2xI_5(x) - x^4(1-1.2x^2) \right. \\ \left. (I_0(x) - I_0(\infty)) \right] = R(x) \quad (7)$$

$$\text{with } P = -x^{-1} - 2x + 2x^2 E' / \Lambda \quad (8)$$

$$Q = x^{-2} - 2(Z + E - 2x^3 E') / \Lambda \quad (9)$$

$$\Lambda = E - xE' \quad (10)$$

$$E = \frac{2}{\pi^{\frac{1}{2}}} \int_0^x \exp(-y^2) dy \quad (11)$$

$$I_n(x) = \int_0^x a_1(y) e^{-y^2} y^n dy \quad (12)$$

where $x = v/v_e$, $v_e = (2T_e/m)^{\frac{1}{2}}$, T_e is the electron temperature, m is the electron mass and Z is the effective plasma charge. Equation (7) is identical with that of Cordey et al [6] except for the driving term $R(x)$ which is found to be

$$R(x) = \left\{ \begin{array}{ll} \frac{12D_C}{v_e^3 v_0 \Lambda} (x^2 - u_0^2)^{\ell-1} u_0 x (u_0^2 + \ell - x^2); & \text{EC} \\ \frac{6D_L}{v_e^3 v_0 \Lambda} [x^3 \delta(x - u_0) - 2u_0^3 x - u_0 x]; & \text{LD} \end{array} \right\} \text{ for } x > u_0 \quad (13)$$

and $R(x) = 0$ for $x < u_0$.

In eq(13)

$$v_o = \frac{4\pi\ell n\Lambda n e^4}{v_e^3 m^2}, \quad \ell n\Lambda \text{ is the Coulomb logarithm, and } n \text{ is the}$$

electron density. The normalised phase velocity u_o is defined by $u_o = (\omega - \ell\omega_c)/k_{||}v_e$ and $u_o = \omega/k_{||}v_e$ for the electron cyclotron (EC) and Landau damping (LD) schemes, respectively. The term $R(x)$ vanishes for $x < u_o$ because electrons with speeds less than the wave phase velocity cannot resonate with the wave. The boundary conditions on the solutions of eq(7) are

$$\begin{aligned} a_1 &\rightarrow cx^3; & \text{EC} \\ a_1 &\rightarrow cx; & \text{LD} \end{aligned} \quad \text{as } x \rightarrow \infty$$

and $a_1 \rightarrow 0$ as $x \rightarrow 0$ for both cases.

The electron current density is given in terms of $I_3(\infty)$ by

$$J = -e\int v_{||} f'_{eo} d^3v = -\frac{4e}{3\pi^{1/2}} v_e n I_3(\infty). \quad (14)$$

A measure of the efficiency of the current drive is the ratio of the current density to the power density, P_d , which is given by

$$P_d = \int \frac{1}{2} m v^2 \left(\frac{\partial f}{\partial t} \right)_w v_{||} dv_{||} dv_{\perp}. \quad (15)$$

The ratio of current density to power density is then given by

$$\frac{J}{P_d} = \frac{2v_e^3 v_o e^{u_o^2}}{3D_c \ell!} I_3(\infty) \quad (16)$$

for the electron cyclotron case and by

$$\frac{J}{P_d} = \frac{2v_e^3 v_o e^{u_o^2}}{3D_L u_o^2} I_3(\infty) \quad (17)$$

for the Landau damping case. The current density is expressed

in units of $-nev_e$ and the power density in units of $nmv_e^2v_o$ following the convention of Fisch^[7]. Note however that the present definitions of v_e and v_o differ from those in ref.7 by factors of $\sqrt{2}$ and $(4\sqrt{2})^{-1}$ respectively. In practical units of amps/watt the total current I per unit power P injected into a tokamak of major radius R and uniform plasma parameters is given by

$$\frac{I(\text{amps})}{P(\text{watts})} = 0.122 \frac{T_e(\text{keV})}{R(\text{m})n_{20}^{\ell n \Lambda}} \cdot \frac{J}{P_d} \quad (18)$$

where the density n_{20} is in units of 10^{20} m^{-3} .

(b) The Lorentz Gas Limit ($Z \gg 1$)

As the plasma effective charge becomes large the electron-ion collisions dominate the electron-electron collisions and an analytic solution of equation 7 is possible. Thus we obtain

$$a_1(x) = \left\{ \begin{array}{ll} \frac{6D_C}{v_e^3 v_o} Z (x^2 - u_o^2)^{\ell-1} u_o x [x^2 - \ell - u_o^2]; & \text{EC} \\ \frac{3D_L}{v_e^3 v_o} Z [(2u_o^3 + u_o) x - x^3 \delta(x - u_o)]; & \text{LD} \end{array} \right\} \text{ for } x \geq u_o \quad (19)$$

and $a_1(x) = 0$ for $x < u_o$.

The solution for the electron cyclotron wave leads to the following expression for J/P_d :

$$J/P_d = \frac{3}{Z\ell!} u_o^2 \int_0^\infty y^\ell (y + u_o^2)^{\frac{1}{2}} e^{-y} dy \quad (20)$$

which has the following forms at small and large u_o :

$$J/P_d \rightarrow \frac{3\pi^{\frac{1}{2}}}{2\ell!} u_o [(\ell+\frac{1}{2})(\ell-\frac{1}{2})\dots\frac{3}{2},\frac{1}{2}] \text{ as } u_o \rightarrow 0 \quad (21)$$

and $J/P_d \rightarrow \frac{3}{2} u_o^2 \text{ as } u_o \rightarrow \infty . \quad (22)$

Thus, the current drive efficiency is a monotonically increasing function of the wave phase velocity with a linear behaviour at low u_o and a quadratic dependence at large u_o .

For the Landau damping scheme we obtain

$$J/P_d = \frac{1}{2Zu_o} \left[3u_o^3 + 3u_o + 3(2u_o^2 + 1)e^{u_o^2} \int_{u_o}^{\infty} e^{-x^2} dx \right] \quad (23)$$

which reduces to

$$J/P_d = \frac{1.33}{u_o Z} \text{ as } u_o \rightarrow 0 \quad (24)$$

and $J/P_d = \frac{4u_o^2}{Z} \text{ as } u_o \rightarrow \infty . \quad (25)$

Consequently currents can be driven with high efficiency at both extremes of u_o in agreement with the calculations of Fisch and Karney^[2,3]. At large u_o the electron cyclotron and Landau damping schemes both drive currents in proportion to u_o^2 and in the ratio of 3:4 which agrees with the estimate of Fisch and Boozer^[4]. Values of J/P_d obtained from eqs(20) and (21) are plotted against u_o^2 in Fig.1 where it can be seen that the above functional dependencies at small and large u_o are maintained in the full solution.

(c) Numerical Solution

The integro-differential equation was solved numerically using the two point boundary value technique described in ref. 6 for values $0.01 \leq u_o^2 \leq 10$, $1 \leq Z \leq 16$ and electron cyclotron

harmonics $\ell=1, 2$ and 3 . The discontinuity at $x=u_0$ was smoothed as in ref.6 and the delta function appearing in $R(x)$ for the Landau damping case was approximated by a gaussian

$$\delta(x-u_0) \sim \frac{1}{\pi^{1/2}\Delta} \exp[-(x-u_0)^2/\Delta^2] \quad (26)$$

with $\Delta \leq 0.05$. This gaussian was also used in the calculation of P_d . In Fig.1 the solid curves show the values of J/P_d plotted against u_0^2 for $Z=1$ and 2 . The Landau damping scheme is always the more efficient but the electron cyclotron scheme becomes competitive at large u_0 . Also shown are the J/P_d values for the third harmonic electron cyclotron wave which is more effective than the lower harmonics at large u_0 but less effective at small u_0 . A comparison with the Lorentz solution (the dotted curves in Fig.1) shows that the electron-electron collisions reduce the efficiency by up to a factor of six for the electron cyclotron wave and by up to a factor of five for Landau damping, the largest reductions occurring at large u_0 . The solid curves for the electron cyclotron wave have been fitted to better than 10% with the expression

$$J/P_d = \alpha_\ell u_0 + \beta_\ell u_0^2. \quad (27)$$

The values of α_ℓ and β_ℓ for $\ell=1, 2$ and 3 and a range of Z values are given in Table 1.

An interesting feature of the Landau damping scheme is that the values of J/P_d approach those given by the Lorentz solution at low u_0 . This can be derived analytically in the following way. For small values of u_0 the particular integral of eq(7) becomes

$$a_1(x) = \frac{3D_L u_0 x}{v_e^3 v_0 Z} \text{ for } x \geq u_0 \quad (28)$$

with $a_1(x) = 0$ for $x < u_0$. The discontinuity in $a_1(x)$ can be removed by adding part of the general solution as described in ref.6. This smoothing makes no contribution to the current which is given by

$$J/P_d = \frac{1.33}{u_0 Z} \quad (29)$$

and is identical with the Lorentz gas value.

The current predicted for Landau damping for $Z=1$ can be compared with the results of the numerical calculation of Fisch and Karney^[3] in which the collision term $C_{ee}(F_m, f_e')$ was omitted and its effect taken into account by using a displaced Maxwellian for the background distribution in the remaining electron-electron collision operator. These authors show that their results can be well represented by the expression

$$J/P_d = 1.4 u_0^{-1} + 0.7 u_0^2 \quad (30)$$

where the coefficients are appropriate to the present definitions of v_e and v_0 . Equation (30) gives good agreement with the present results at $u_0 = 0.1$ but underestimates the current by 20% at $u_0=3$.

The dependence of J/P_d on plasma charge is shown in Fig.2 where the ratio $J(Z)/J(1)$ is plotted against Z for $u_0 = 0.1$ and 3. For $u_0 = 3$ this ratio approaches the $(Z+5)^{-1}$ dependence derived

by Fisch and Boozer^[4] while for smaller values of u_0 the variation is stronger, with the Landau damping scheme showing the z^{-1} variation given by eq(29).

3 THE EFFECT OF TRAPPED ELECTRONS

In this section the reduction in wave driven current produced by trapping of the electrons is investigated for plasmas in the banana regime of collisionality.

(a) General Treatment for Large Aspect Ratios

In the conventional neoclassical theory of Rosenbluth et al^[8] and Hazeltine et al^[9] the perturbed electron distribution function f'_e , to order $\epsilon^{\frac{1}{2}}$ in the inverse aspect ratio ($\epsilon=r/R$), is written in terms of f'_{e0} , the perturbed distribution for no trapping, as

$$f'_e = f'_{e0} + h^0 + f^* \quad (31)$$

where h^0 is the part of the distribution function which is localised in the trapped particle region and f^* takes account of the friction between the trapped and passing electrons^[9]. The function f'_e satisfies the Fokker-Planck equation

$$\left(\frac{\partial f_e}{\partial t} \right)_w + C_{ei}(f'_e, F_m) + C_{ee}(f'_e, F_m) + C_{ee}(F_m, f'_e) = \frac{\xi v}{r} \frac{B_\theta}{B_\phi} \frac{\partial f'_e}{\partial \theta} \quad (32)$$

where B_θ/B_ϕ is the ratio of the poloidal and toroidal fields respectively and $\left(\frac{\partial f_e}{\partial t} \right)_w$ is given by eqs(2) and (3) for the electron cyclotron and Landau damping schemes respectively. The functions h^0 and f^* are now expressed in terms of Legendre polynomials

$$h^0 = F_m \sum_n h_n^0(v, \theta) P_n(\xi) \text{ and } f^* = F_m \sum_n f_n^*(v, \theta) P_n(\xi). \quad (33)$$

Substituting eq(31) into eq(32) and taking flux surface averages leads an integro-differential equation, analogous to eq(7), for the first order coefficients^[10]

$$b_1'' + P(x)b_1' + Q(x)b_1 = \frac{16}{3\pi^{1/2}\Lambda} [xI_3(x) - 1.2xI_5(x) - x^4(1-1.2x^2)(I_0(x) - I_0(\infty))] = R(x) \quad (34)$$

$$\text{where } b_1 = \langle h_1^0 \rangle + \langle f_1^* \rangle \quad (35)$$

$$\text{and } R(x) = \frac{\langle h_1^0 \rangle}{\Lambda x^2} [xE' + (2x^2-1)E + 2Zx^2] \quad (36)$$

in which the triangular brackets denote flux surface averages. The localised function $\langle h_1^0 \rangle$ is now obtained in terms of f_{e0}' using the constraint equation of ref.9 which ensures that the trapped part of the electron distribution function is an even function of ξ . However unlike the steady electric field case treated in ref.9, the resonant wave-electron interactions generate Legendre polynomial terms in f_{e0}' of higher order than $P_1(\xi)$. This can be seen from the coefficients $a_n(x)$ for the Lorentz gas:

$$a_n(x) = \begin{cases} \frac{8D_c}{v_e^3 v_o^Z} \frac{(n+1/2)}{n(n+1)} x^2 (x^2 - u_o^2)^{\ell-1} [x^2 - u_o^2 - \ell] P_n(u_o/x); & \text{EC} \\ \frac{4D_L}{v_e^3 v_o^Z} \frac{(n+1/2)}{n(n+1)} [2x^2 u_o^2 P_n(u_o/x) + x u_o P_n'(u_o/x) - \delta(x - u_o) x^3]; & \text{LD} \end{cases} \quad \text{for } x > u_o \quad (37)$$

with $a_n(x) = 0$ for $x < u_o$ for both schemes. The slow, n^{-1} variation of these coefficients means that the higher order terms must be taken into account. In this case the solution to the zeroth order constraint equation of ref.9 becomes

$$\frac{\partial h_o}{\partial \lambda} = F_m \left[\frac{\sigma}{2} \frac{\sum_n a_n P_n'}{\left(\frac{1-\lambda B}{B}\right)^{1/2}} - \frac{\sigma}{2} \frac{\left\langle \sum_n a_n P_n' \right\rangle}{\left\langle \left(\frac{1-\lambda B}{B}\right)^{1/2} \right\rangle_p} - \frac{\left\langle \sum_{\text{even } n} a_n P_n' \right\rangle}{\left\langle \left(\frac{1-\lambda B}{B}\right)^{1/2} \right\rangle_t} \right] \quad (38)$$

where $\sigma = v_{||} / |v_{||}|$, $\lambda = v_{\perp}^2 / v^2 B$, B is the total magnetic field, the argument of the Legendre polynomials is $\sigma(1-\lambda B)^{1/2}$ and the subscripts p and t refer to passing and trapped electrons respectively. Equation (38) can now be used to obtain $\langle h_1^O \rangle$ using the expression

$$\langle h_1^O \rangle_{F_m} = \frac{3}{2} \int_{-1}^{+1} \frac{d\theta}{2\pi} h_O P_1(\xi) d\xi. \quad (39)$$

Changing variables from ξ to λ and integrating by parts gives

$$\langle h_1^O \rangle = -a_1 + \sum_{n_{\text{odd}}} a_n H_n \quad (40)$$

$$\text{where } H_n = \frac{3}{4} \langle B \rangle \int_0^{1/B_{\text{max}}} \lambda d\lambda \frac{\langle P_n'[(1-\lambda B)^{1/2}] \rangle}{\langle \frac{(1-\lambda B)^{1/2}}{B} \rangle}. \quad (41)$$

The integrals H_n have been evaluated numerically for the tokamak field configuration, $B = B_0(1-\epsilon \cos \theta)^{-1}$ and are shown in Fig.3 as a function of ϵ for $n \leq 9$.

The electron current is given by

$$\langle J \rangle = -\frac{4ev_e n}{3\pi^{1/2}} I_{3\text{tot}} \quad (42)$$

$$\text{where } I_{3\text{tot}} = \int_0^{\infty} (a_1 + b_1) x^3 e^{-x^2} dx. \quad (43)$$

Thus the current can be determined once eq(34) has been solved for b_1 using eq(40) to obtain $\langle h_1^O \rangle$ which appears in the driving term, $R(x)$. Determination of $\langle h_1^O \rangle$ requires all the coefficients $a_n(x)$ for the solution without trapping to be obtained from integro-differential equations similar to eq(7). This complete

treatment is beyond the scope of the present paper, but calculations are given below for the Lorentz gas case for which the coefficients $a_n(x)$ are known analytically.

(b) The Lorentz Gas Limit ($Z \gg 1$)

In this limit the electron-electron collision term is negligible compared with the electron-ion collision term and the first order constraint equation of Hazeltine, Hinton and Rosenbluth^[9], which determines the localised distribution function h^0 , becomes the exact constraint equation. Thus for the Lorentz gas case the perturbation of the electron distribution function is given by

$$f'_e = f'_{e0} + h^0 \quad (44)$$

and the vanishing of f^* and higher order terms removes the restriction of the calculation to small values of ϵ . The result $\langle f^* \rangle = 0$ can also be seen from eq(34) as $Z \rightarrow \infty$.

The total electron current is given by substituting eq(40) into eq(42) which becomes

$$\langle J \rangle = - \frac{4ev_e n}{3\pi^{\frac{1}{2}}} \int_0^\infty x^3 e^{-x^2} dx \sum_{n_{\text{odd}}} a_n(x) H_n \quad (45)$$

with the $a_n(x)$ given by eq(37).

Normalising to unit power density we obtain:

$$\frac{\langle J \rangle}{P_d} = \left\{ \begin{array}{l} \frac{16e}{3Z\ell!} \sum_{n_{\text{odd}}} \frac{(n+\frac{1}{2})}{n(n+1)} H_n \int_{u_0}^\infty x^5 e^{-x^2} (x^2 - u_0^2)^{\ell-1} \left\{ u_0^2 + \ell - x^2 \right\} P_n\left(\frac{u_0}{x}\right) dx; \text{ EC} \\ \frac{8e}{3Zu_0^2} \sum_{n_{\text{odd}}} \frac{(n+\frac{1}{2})}{n(n+1)} H_n \int_{u_0}^\infty x^3 e^{-x^2} \left\{ x^3 \delta(x-u_0) - 2x^2 u_0^2 P_n\left(\frac{u_0}{x}\right) - x u_0 P'_n\left(\frac{u_0}{x}\right) \right\} dx; \text{ LD} \end{array} \right\} \quad (46)$$

The integrals appearing in eq(46) were evaluated numerically and curves of $\langle J \rangle \cdot Z/P_d$ versus u_0 for $\epsilon=0, 0.03$ and 0.1 are shown in Figs. 4 and 5 for the electron cyclotron and Landau damping schemes respectively. At high values of u_0 the electron trapping for $\epsilon=0.1$ reduces the current by a factor of two in the case of the electron cyclotron wave and by a factor of $3/2$ for Landau damping. At these high phase velocities most of the electrons interacting with the wave have large values of $v_{||}/v$ and are passing particles so that the diminution of current is relatively modest.

At low phase velocity the trapped electrons effectively destroy the current. Physically this is because the current is being carried by electrons of low parallel velocity and so only small increases in $v_{||}$, due to wave-induced diffusion or collisions, are sufficient to trap these electrons. For the Landau damping case, the curves shown in Fig.5 for $u_0^2 < 10^{-1}$ also apply when electron-electron collisions are important since, in this region of phase velocity, the electron distribution function for no trapping, f'_{eo} , is identical with that for the Lorentz gas.

The dashed curves in Figs.4 and 5 show the effect on the Lorentz gas calculation of using only the $P_1(\xi)$ term in f'_{eo} and, for the high values of u_0 , give a reasonable approximation to the results obtained using the full Legendre expansion. With such a truncated electron distribution function we can also solve numerically the full Fokker Planck equation (eq(34)) as described in section 3(a) to investigate the effect of the electron-electron collisions. The results of this calculation are shown in Fig.6

where the dashed curves are the values of J/P_d for $\epsilon=0.1$ and the solid curves for $\epsilon=0$ (no trapping). Comparison with the corresponding curves in Figs.4 and 5 shows that at $u_0^2=10$, the electron-electron collisions approximately halve the percentage reduction in current caused by the trapped electrons. At $u_0^2=1$ however the electron-electron collisions have much less effect and, for Landau damping, even increase the percentage loss of current.

4 COMPARISON WITH OTHER CURRENT GENERATING SCHEMES

In this section we compare the efficiency of driving currents by means of the electron cyclotron and Landau damping schemes with that obtained using (a) an idealised wave, (b) fast ion beams and (c) steady electric fields (ohmic heating).

To investigate how the wave-driven current scheme might be optimised we consider a wave which causes parallel velocity diffusion and interacts with the electrons at a specific point in velocity space. The co-ordinates, ξ_0 and v_0 , of this point of interaction are then varied to maximise the value of J/P_d . The driving term is taken to be:

$$\left(\frac{\partial f_e}{\partial t}\right)_w = \frac{\partial}{\partial v_{||}} \left[D_i \delta(\xi - \xi_0) \delta(v - v_0) \frac{\partial F_m}{\partial v_{||}} \right] \quad (47)$$

which gives

$$R(x) = \frac{6D_i}{v_e^3 v_0 \Lambda} \left[\xi_0^3 x^4 \delta(x - u_0) - \xi_0^3 (2x^2 - 1) x^3 \delta(x - u_0) + 3(\xi_0^2 - 1) \xi_0 x^3 \delta(x - u_0) \right] \quad (48)$$

where $u_0 = v_0/v_e$.

Approximating the delta function by a gaussian as in eq(26) and numerically solving eq(7) leads to the J/P_d values shown in Fig.7 as a function of both ξ_0 and u_0 . Clearly the greatest efficiency is obtained when the wave interacts with high energy electrons with small parallel velocity components. For $\xi_0=0.1$ and $u_0=3$ the efficiency is approximately an order of magnitude greater than that of both the electron cyclotron and Landau damping schemes at the same value of u_0 (see Fig.1). Thus these two practical methods are relatively inefficient compared to the inherent potential of the wave-drive mechanism which has an optimum efficiency comparable with that achieved with steady electric fields (see Fig.8).

The efficiency of driving current using fast ion beams with velocity $v_b \ll v_e$ is given by^[10]

$$J/P_d = \frac{3\pi^{1/2}K_1}{2u_0 Z_b (1+\alpha^3)} (1-Z_b/Z + 1.46\epsilon^{1/2}AZ_b/Z) [1+(3-2\alpha^2\beta)\delta/(1+\alpha^3)]^2 \times \int_0^1 x^{3+\beta} \left(\frac{1+\alpha^3}{x^3+\alpha^3} \right)^{1+\beta/3} dx \quad (49)$$

where $\alpha^3 = 0.75\pi^{1/2}m(\sum n_i Z_i^2 / mn) / u_0^3$,

$\beta = m_i Z / m_b$, $\delta = T_e / 2\epsilon_0$, $u_0 = v_b / v_e$, ϵ_0 is the injection energy, K_1 is the first order co-efficient in the Legendre polynomial expansion of the fast ion angular distribution, n_b , m_b and Z_b are the density, mass and charge of the fast ions respectively and n_i , m_i and Z_i the corresponding quantities for the plasma ions. Values of J/P_d calculated using eq(49) are plotted against u_0^2 in Fig.8 for deuterium, helium and oxygen ion beams injected into a mixed D,T plasma. Comparison with the results obtained for the electron cyclotron and Landau damping schemes shows the optimum currents driven by

both the ion beams and waves to be of similar magnitude for equal power deposited in the plasma. This conclusion is not significantly modified by the presence of trapped electrons as illustrated by the dashed curves which were obtained from the solution of the full Fokker Planck equation with $\epsilon=0.1$ and only the $P_1(\xi)$ term retained in f'_{e0} .

The top curve in Fig.8 gives the current driven by a steady electric field which was obtained from the expression

$$J/P_d = \frac{8\gamma}{\pi^{1/2} v_d^* Z} \quad (50)$$

where $v_d^* = 3.3 \times 10^{-6} I/n_{20} T_e^{1/2} \pi a^2$ with the plasma current I in kA, T_e in keV, and the minor radius, a , in metres. The quantity γ is the usual Spitzer resistivity correction factor^[11]. For a given total plasma current, v_d^* is inversely proportional to plasma density so that the efficiency (in our particular units) for ohmic heating current drive increases for increasing density, a scaling not shared by the other schemes. The particular curve shown in Fig. 8 is for $v_d^* = 10^{-2}$ which is typical of the DITE tokamak. Larger devices operating at higher temperatures and densities tend to have smaller values of v_d^* giving efficiencies far in excess of those calculated for either the wave or beam driven currents.

5 SUMMARY

In this paper the plasma current driven by radio frequency waves has been calculated for the cases of wave absorption by (a)

Landau damping and (b) electron cyclotron damping. It has been shown that at high phase velocity the two schemes give comparable efficiencies whereas, at low phase velocity, Landau damping is the more effective with J/P_d scaling as u_o^{-1} compared with J/P_d scaling as u_o for the electron cyclotron case. The electron-electron collisions were taken into account using the full Fokker Planck collision operator and have been shown to reduce the current obtained in the Lorentz gas approximation by up to a factor of six at high phase velocities. The reason for this is that the like-particle collisions, whilst not removing momentum from the distribution as a whole, cause the momentum to be transferred to electrons which are slower than those in resonance with the wave. These slower electrons then lose the momentum more readily by collisions with the ions.

The reduction of the current due to trapping of electrons in the field gradient of a tokamak has been found to be particularly effective at low phase velocity where the current is almost entirely suppressed. This is due to the fact that only small increases in perpendicular velocity are required to move electrons from the untrapped to the trapped region of velocity space. At high phase velocity the wave interacts mainly with passing particles and so the reduction in current is more modest.

In comparison with other methods of driving plasma currents, the radio-frequency waves of the present study are as efficient as ion beams but much less efficient than steady electric fields. There is, however, room to improve the wave-drive efficiency as shown by the calculations for the idealised wave.

TABLE 1

VALUES OF α_ℓ AND β_ℓ IN EQUATION 27

	Z=1	2	4	8	16
α_1	1.5	1.4	0.65	0.37	0.20
β_1	0.06	0.13	0.14	0.13	0.09
α_2	1.05	1.0	0.66	0.40	0.21
β_2	0.14	0.17	0.17	0.13	0.10
α_3	1.4	1.0	0.70	0.45	0.27
β_3	0.16	0.19	0.17	0.13	0.08

REFERENCES

- 1] WORT D J H, Plasma Physics 13 (1971) 258.
- 2] KARNEY C F F and FISCH N J, Phys.Fluids 22 (1979) 1817
- 3] FISCH N J and KARNEY C F F, Princeton Plasma Physics Laboratory Report No PPPL-1624 (1979) unpublished.
- 4] FISCH N J and BOOZER A H, Phys.Rev.Letters 45 (1980) 720.
- 5] KENNEL C F and ENGLEMAN F, Phys.Fluids 9 (1966) 2377.
- 6] CORDEY J G, JONES E M, START D F H, CURTIS A R and JONES I P, Nuclear Fusion 19 (1979) 249.
- 7] FISCH N J, Phys.Rev.Letters. 41 (1978) 873.
- 8] ROSENBLUTH M N, HAZELTINE R D and HINTON F L, Phys.Fluids 15 (1972) 116.
- 9] HAZELTINE R D, HINTON F L and ROSENBLUTH M N, Phys.Fluids 16 (1973) 1645.
- 10] START D F H, CORDEY J G and JONES E M, Plasma Physics 22 (1980) 303.
- 11] SPITZER L and HARM R, Phys.Rev. 89 (1953) 977.

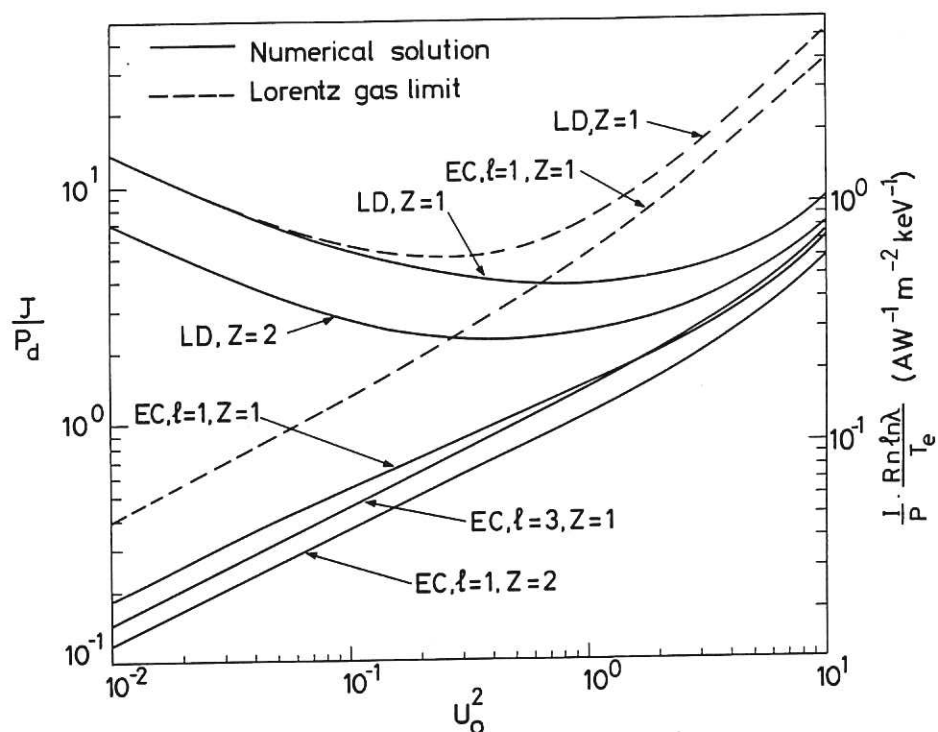


Fig.1 Current density per unit power density, J/P_d , as a function of u_0^2 for the electron cyclotron and Landau damping schemes. The continuous curves show the results obtained using the full Fokker-Planck collision operator for $Z = 1$ and 2 , and for electron cyclotron harmonics $\ell = 1$ and 3 . The dashed curves are the results obtained using the Lorentz approximation. The scale on the right facilitates conversion to total current (amps) per unit power (watts) injected into a tokamak of major radius R . The density, n , is in units of 10^{20} m^{-3} .

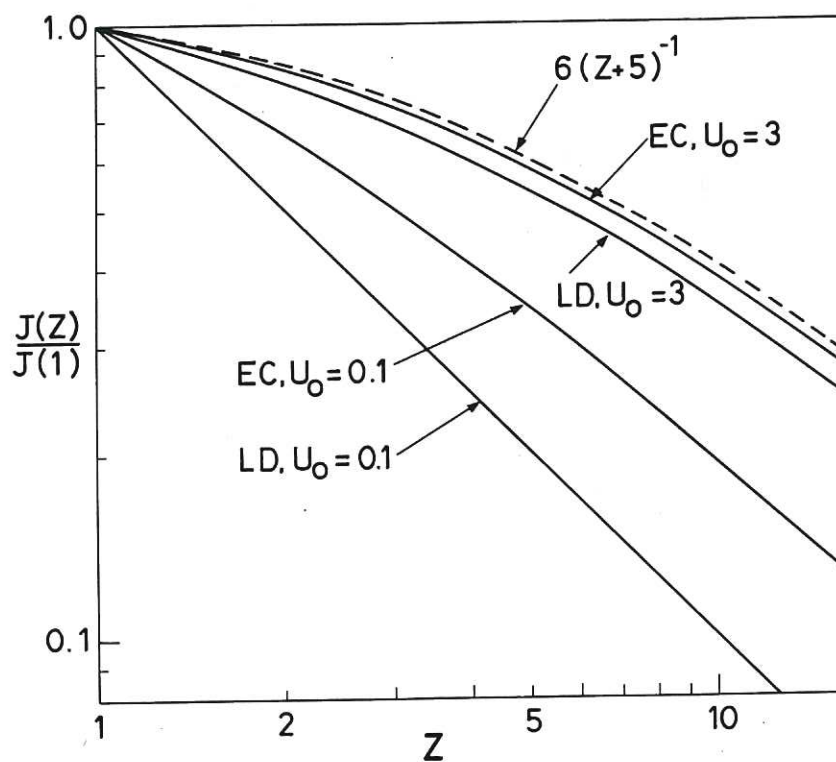


Fig.2 Functional dependence of the current on plasma charge Z for both high phase velocity ($u_0 = 3$) and low phase velocity ($u_0 = 0.1$). The dashed curve shows the functional form given in Ref.4.

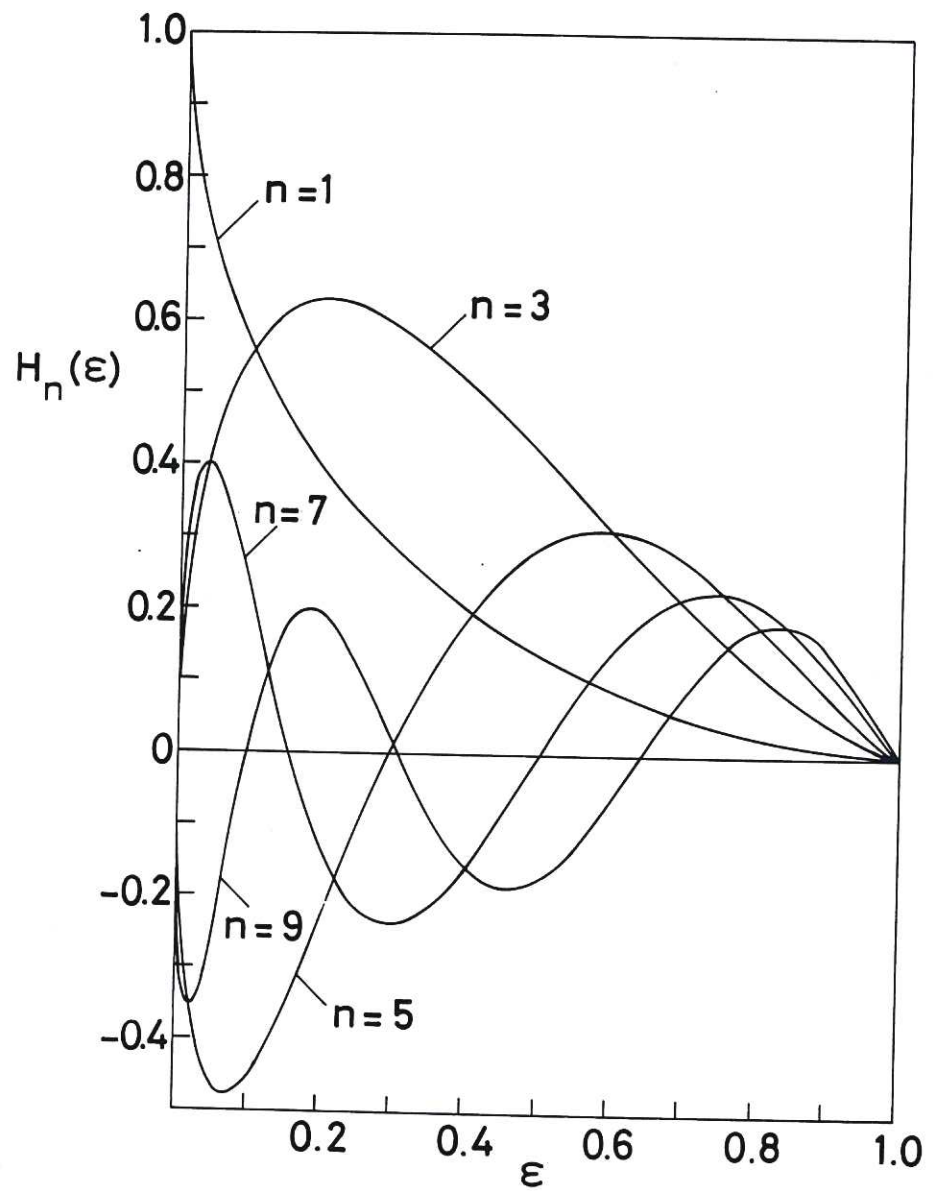


Fig.3 Integrals H_n given by Eq.(41) as a function of the inverse aspect ratio ϵ for $n \leq 9$.

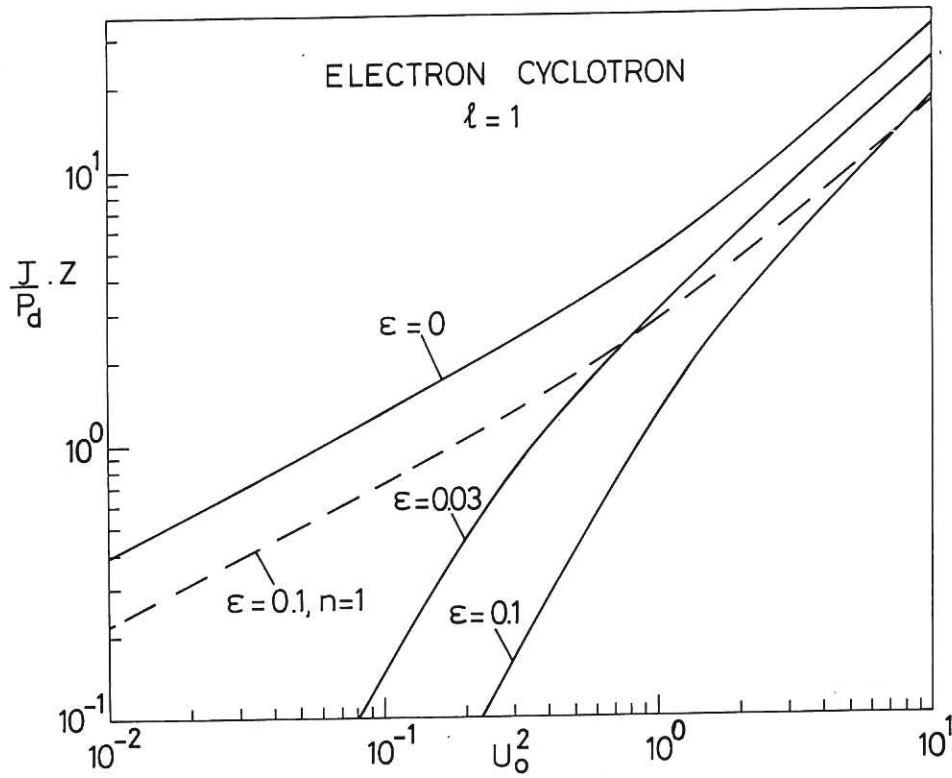


Fig.4 Current density per unit power density times Z as a function of u_0^2 for electron cyclotron heating with trapped electrons present in tokamak field geometry. The continuous curves show the current calculated in the Lorentz approximation for $\epsilon = 0, 0.03$ and 0.1 . The dashed curve shows the effect of using only the $n = 1$ term in Eq.(46).

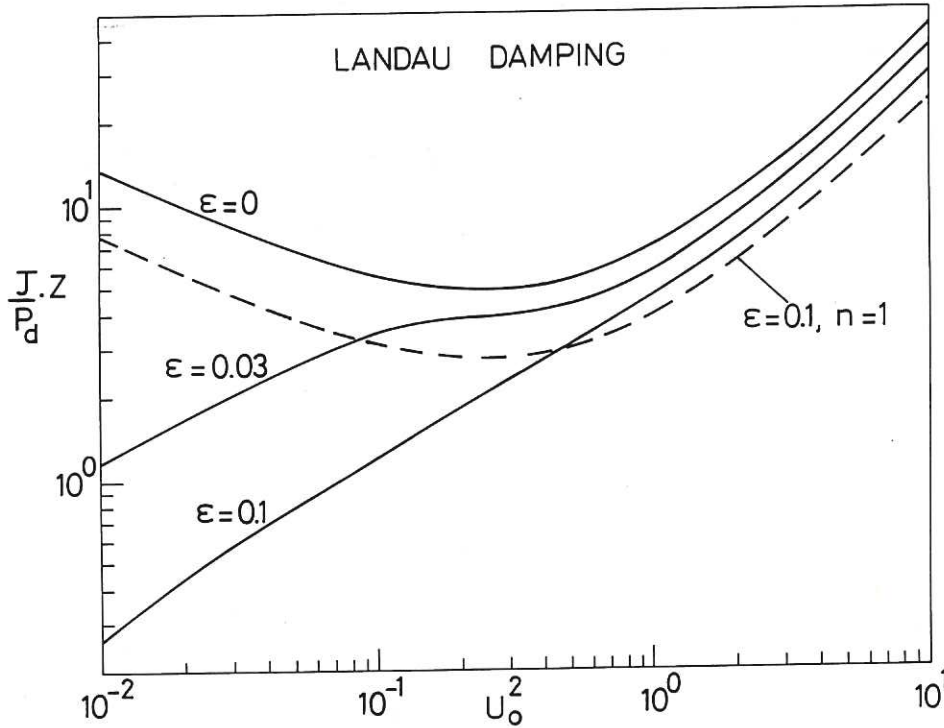


Fig.5 Current density per unit power density times Z as a function of u_0^2 for the Landau damping scheme with trapped electrons present in tokamak field geometry. The continuous curves show the current calculated in the Lorentz approximation for $\epsilon = 0, 0.3$ and 0.1 . The dashed curve shows the effect of using only the $n = 1$ term in Eq.(46).

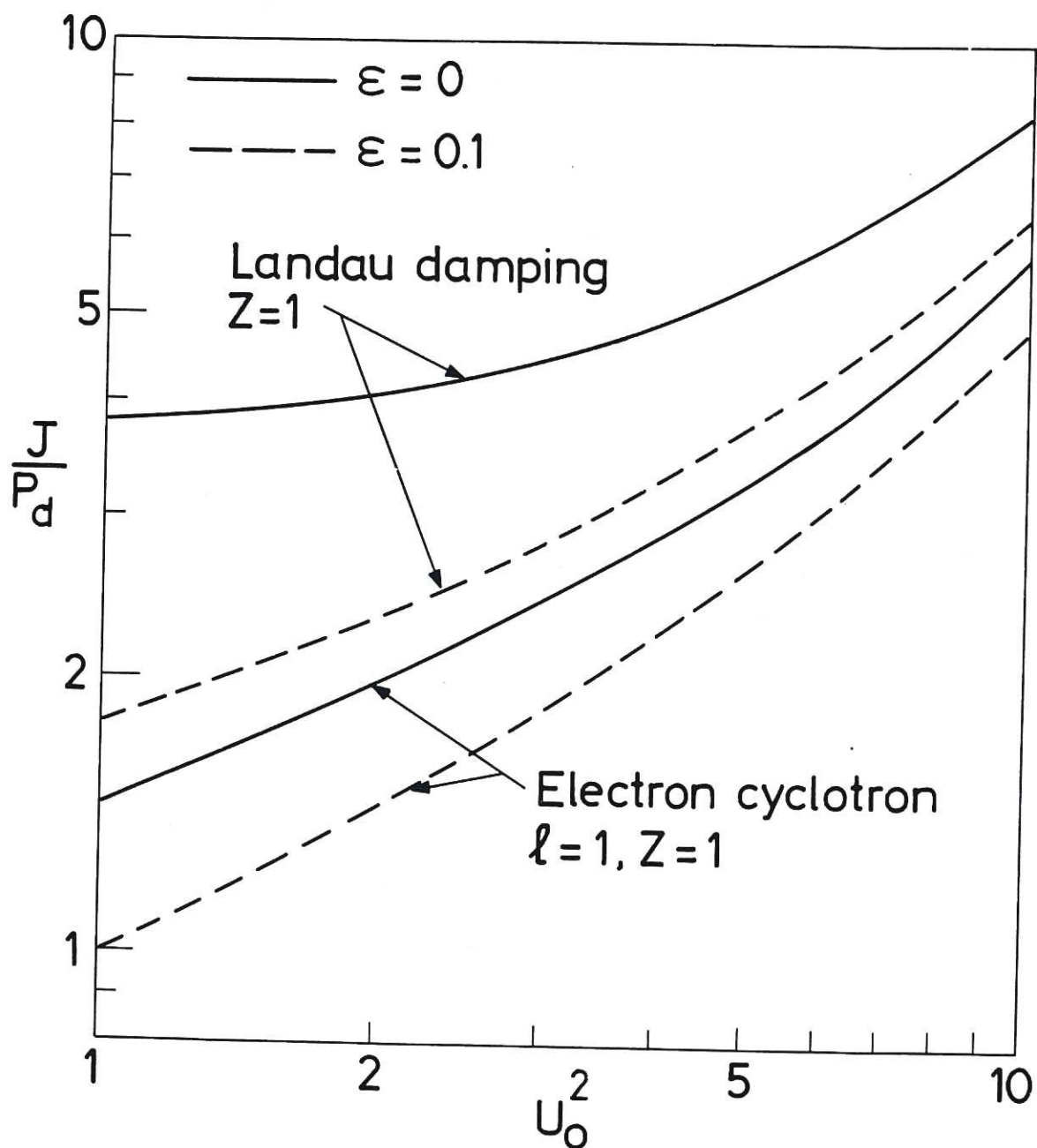


Fig.6 Current density per unit power density versus u_0^2 at high phase velocity with the solid curves showing the current for no electron trapping. The dashed curves for $\epsilon = 0.1$ were calculated using the full Fokker-Planck equation but retaining only the $n = 1$ term in Eq.(40).

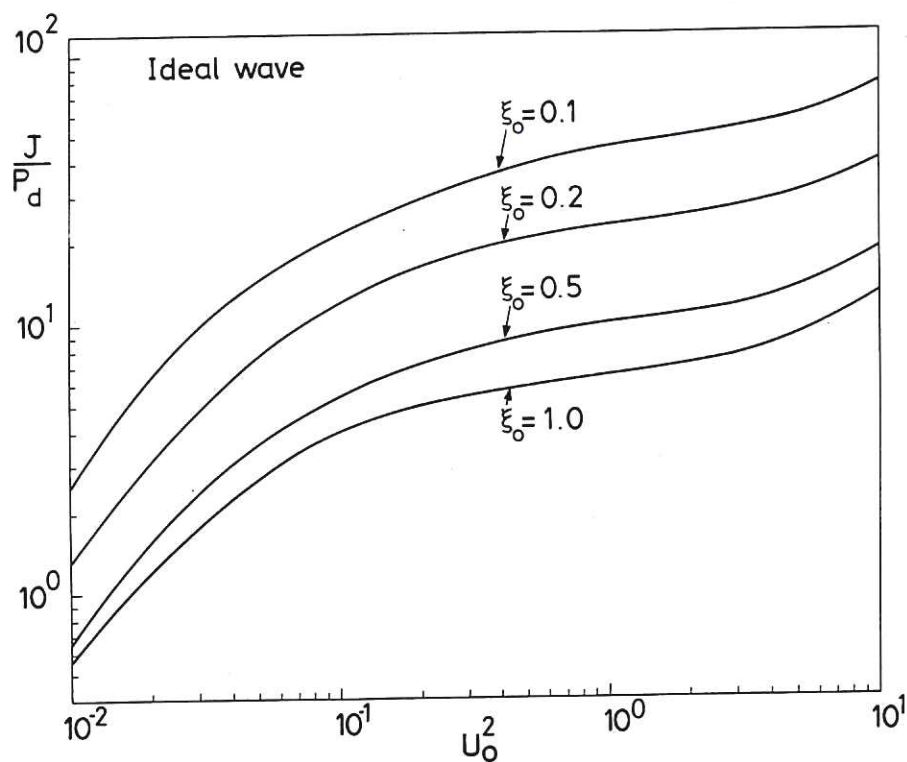


Fig.7 Current density per unit power density as a function of u_0^2 for an idealised wave interacting with a plasma according to Eq.(47).

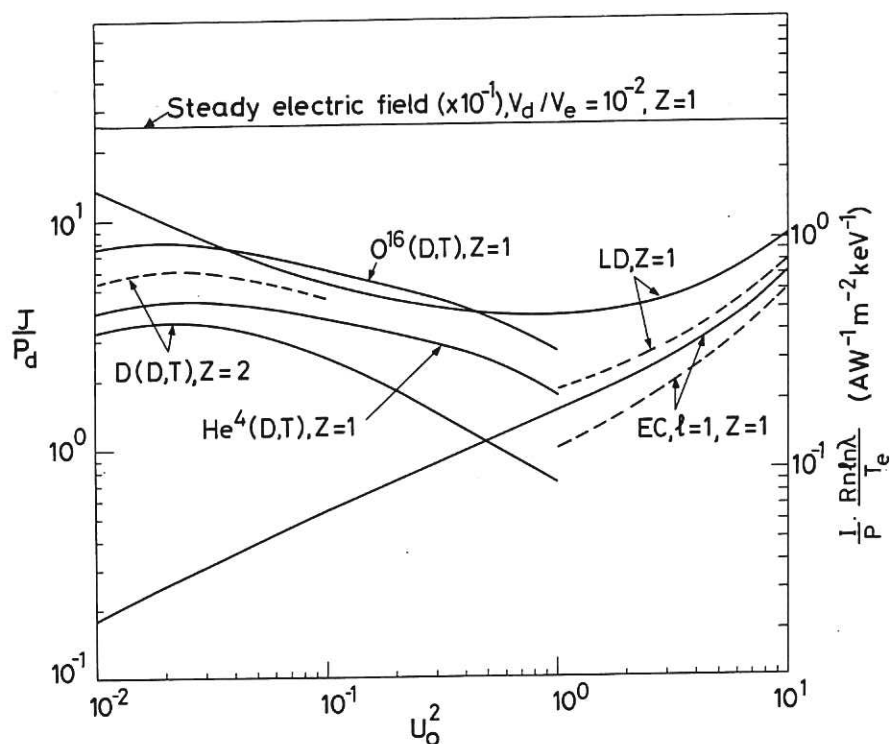


Fig.8 Comparison of the efficiencies for generating current using waves, ion beams and steady electric fields. The continuous curves are for no electron trapping and the dashed curves include trapping with $\epsilon = 0.1$. The scale on the left gives J/P_d while the scale on the right facilitates conversion to total current (amps) per unit power (watts) injected into a tokamak of major radius R . Note that the value of J/P_d for the steady electric field has been scaled down by a factor of ten.



